Thermodynamics analysis of CO_2 condensation in supersonic flows for the potential of a clean offshore natural gas processing

Chuang Wen[1], Bo Li[2], Hongbing Ding[3], Mohammad Akrami[1], Haoran Zhang[4], Yan Yang[5,*]

[1]College of Engineering, Mathematics and Physical Sciences, University of Exeter, Exeter EX4 4QF, UK

[2]School of Engineering, University of Kent, Kent CT2 7NZ, UK

[3]School of Electrical and Information Engineering, Tianjin University, Tianjin 300072, China

[4]Center for Spatial Information Science, The University of Tokyo, 5-1-5 Kashiwanoha, Kashiwa, Chiba 277-8563, Japan

[5]Faculty of Engineering, University of Nottingham, Nottingham NG7 2RD, UK

*Email: yan.yang1@nottingham.ac.uk

Abstract: Carbon capture and storage technology are thought as promising methods to global climate change challenges. The separation technology of carbon dioxide (CO_2) is a key step to achieve high efficient carbon capture and storage target. The conventional CO_2 separation technologies including cryogenics, adsorption, absorption and membranes are proven to be costly with potentially hazardous chemicals involved. In the present study, we propose a new concept to remove CO_2 from the offshore natural gas industry, which utilises the combined effect from nonequilibrium condensation phenomena in the supersonic flow and cyclonic separation process from induced swirling flows. The feasibility study of this concept is evaluated by using computational

The short version of the paper was presented at ICAE2020, Dec 1-10, 2020. This paper is a substantial extension of the short version of the conference paper.

fluid dynamics modelling. The effect of thermodynamics properties on the phase change process in the supersonic flows is analysed in detail. The results show that the supersonic flow can condense 28% CO_2 in a liquid state from the main gas flow based on the real gas model. Nine orders of magnitude differences are observed between the mass generations due to the nucleation process and the droplet growth process, which indicates that the droplet growth process contributes more significantly to the mass transfer during CO_2 condensations. The ideal gas model both under-predicts the mass flow rate and the liquid fraction by 25% and 46% compared to the real gas model. This study demonstrates the potential application of the CO_2 separation using the phase change behaviour in supersonic flows.

Keywords: Thermodynamics, carbon dioxide, separation, carbon capture, condensation, CO_2, carbon emission

Nomenclature

CCS	carbon capture and storage	r	droplet radius, m
CFD	computational fluid dynamics	r_c	critical droplet radius, m
SST	shear stress transport	T	temperature, K
Cp	specific heat at constant	u	velocity, m · s^{-1}
	pressure, J K^{-1}	x	Cartesian coordinates, m
E	total energy, J kg^{-1}	y	liquid fraction, -
h_{lv}	latent heat, J kg^{-1}	α	modelling parameter, -
I	nucleation rate, m^{-3} s^{-1}	β	modelling parameter, -
k	turbulence kinetic energy, m^2 s^{-2}	γ	specific heat ratio, -
k_B	Boltzmann's constant, 1.38×10^{-23}	λ_v	vapour conductivity, W · m^{-1}·K^{-1}
	J K^{-1}	v	modelling correction coefficient, -
Kn	Knudsen number, -	ρ	density, kg m^{-3}
Ldr	condensation loss, MW	σ	surface tension, N · m^{-1}
$\dot{m}$	condensation mass generation	τ_{ij}	viscous stress tensor, kg m^{-1} s^{-2}
m_v	rate, kg m^{-3} s^{-1}	ϕ	temperature correction
n	mass of a vapour molecule, kg		coefficient, -
p	droplet number per volume, m^{-3}	ω	specific dissipation rate, s^{-1}
Pr	pressure, Pa		Subscript
q_c	Prandtl number, -	c	critical condition
q_{jeff}	condensation coefficient, -	i, j	Cartesian tensor notation
r	effective heat flux, W m^{-2}	l	

R_v	radius, m	s	liquid phase
t	gas constant, $J \cdot K^{-1} \cdot mol^{-1}$	v	saturation condition
	time, s		vapour phase

1 Introduction

Carbon capture and storage (CCS) provides an opportunity to mitigate carbon emissions from fossil energies to tackle climate change [1, 2]. The separation technology of carbon dioxide (CO_2) is one of key processes to achieve effective CCS [3, 4]. Strong demands from infrastructural and chemical industries, such as the gas industry [5], iron and steel [6], cement factories [7], and power plants [8], make it imperative to mitigate the environmental impact from its CO_2 emission.

A number of separation technologies have been used for CO_2 removals, such as cryogenics [9], absorption [10], adsorption [11] and membranes [12]. The cryogenic separation technology uses the compression and cooling processes to achieve the phase change of CO_2. The cryogenic separation process takes full advantage of pure physic processing without involving any chemicals in CO_2 capture [13]. The disadvantage includes the possible blockage issue due to the ice formation if the water contents exist in the mixture [14]. The absorption technology is used to separate CO_2 based on physical or chemical processes [15]. The nanofluids were introduced to enhance the absorption process [16]. The adsorption process removes CO_2 from mixtures due to the strong intermolecular effects to adhere the molecular to the surface of a selected material [17]. The adsorption separation technology can be divided into pressure, temperature, electrical swing processes. In membrane techniques, CO_2 is selectively removed from mixtures by means of separation or absorption process [18]. These conventional technologies show considerable performance for the onshore facilities, but it is extremely challenging technically to extend the offshore gas industry due to the limited space, rigorous safety measures and reliabilities.

Supersonic separation is an emerging technology to remove CO_2 from mixtures using the phase change phenomenon in supersonic flows. Cao et al. performed CO_2 condensation modellings within supersonic flows considering the mixture of CH_4-CO_2 [19] and CH_4-H_2S-CO_2 [20], respectively. Jiang et al. carried out numerical simulations of CO_2 condensation in supersonic nozzles, including the effect of operating parameters [21], the profile of nozzle converging part [22], and swirling flows [23] on the phase change process. Chen et al. [24] numerically evaluated the effect of the nozzle exit area on the CO_2 condensation based on the mixture of CH_4-CO_2. They found that a larger nozzle exit area increased the liquefaction efficiency but decreased the separation efficiency. These studies made pioneering attempts to reveal the CO_2 phase change phenomenon in gas mixtures, while some mechanisms remain unsolved, such as the diffusion coefficient of CO_2 in the carrier gas of CH_4 and the solubility of the carrier gas in the condensed liquid. Unlike the two-phase flow model for the nonequilibrium condensation, Vijayakumaran and Lemma [25] developed the metastability method to study the phase change of natural gas, which was based on the single-phase flow model and thermodynamic properties. They assumed that the phenomenon of phase change took place in the supersonic nozzle if the pressure and temperature exceeded the CO_2 saturation state. However, a validation of the metastability method was not involved in this paper, and the results need to be further verified against experimental data. Jiang et al. [26] also tracked liquid phase trajectories and subsequently to calculate the separation efficiency for CO_2 removal. In their numerical studies, the droplet sizes were assumed and released in the gas flow, which were not calculated based on the modelling of the nonequilibrium condensation process.

The purpose of this study is to evaluate the effect of the thermodynamics properties on the CO_2 phase change phenomenon inside supersonic flows, which contributes to carbon captures in a cleaner way. We develop a nonequilibrium condensing flow model to improve an accurate prediction of the liquid generation based on two-phase flow modellings. A comprehensive analysis is carried out to evaluate the role of the thermodynamic performance in the complicated condensation process, which not only significantly influences the mass flow rates of the gas mixture, but also harvest a better understanding of the two-phase flow structures in high-pressure supersonic flows. The main contribution of this study is to provide a comprehensive technical option for environmentally-friendly carbon capture and storage.

2 Problem statement

A new concept for CO_2 capture from gases is proposed using nonequilibrium condensations and cyclonic separation in supersonic flows, as shown in Fig. 1. This new concept consists of a Laval nozzle, a set of static vanes and a diffuser. The nozzle is expected to condense CO_2 into liquid droplets from main gases due to the high expansion of the gas mixture in the diverging part, which will be removed due to the strong centrifugal force generated by the static vanes. The diffuser is proposed to recover the static pressure to ensure efficient utilisation of the energy. This new concept achieves CO_2 capture and energy conversion in a clean way due to the pure physical separation process without any chemicals involved, and no pollutant by-products are expected to discharge to our environment.

As depicted in Fig. 2, to concentrate on the nonequilibrium condensation phenomenon of CO_2, a Laval nozzle is deployed in our study as a geometrical basis, which is numerically simulated without the static vanes and diffusers. In the initial design, the Laval nozzle consists of two straight lines and the detailed dimension is listed in Table 1. However, the numerical analysis shows that the intersection angle between these two lines leads to strong shock waves. Therefore, geometry optimisation was processed by using an arc to smoothly connect the converging and diverging parts to form the transonic profile of the Laval nozzle. The radius of the arc is 200.00 mm with the centre point at x = 107.49 mm, y = 212.50 mm. In the optimised Laval nozzle, the throat locates at x = 107.49 mm. Fig. 2 shows the quadrilateral meshes for the Laval nozzle in this numerical study. Furthermore, at the first step of the numerical modelling, it is assumed that pure CO_2 was used to assess the effect of thermodynamic properties on the nonequilibrium condensation of CO_2 in supersonic flows. In other words, the multiple components either for natural gas or flue gas are not considered in this study. As this study is designed for CO_2 removal from offshore natural gas processing, inlet pressure at 40 bar is set in our simulation considering the practical CO_2 removal application. The detailed operating conditions including pressure and temperature for the numerical simulation are described in Table 2.

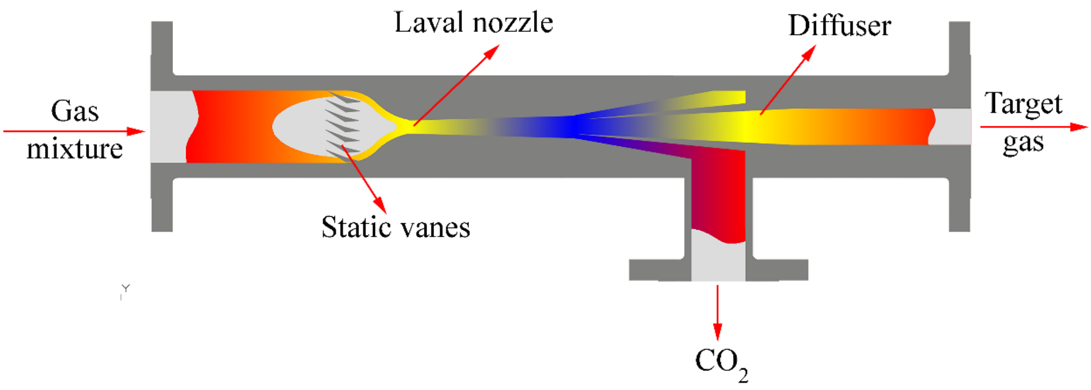

Fig. 1 A new concept of CO_2 capture from gases in supersonic flows

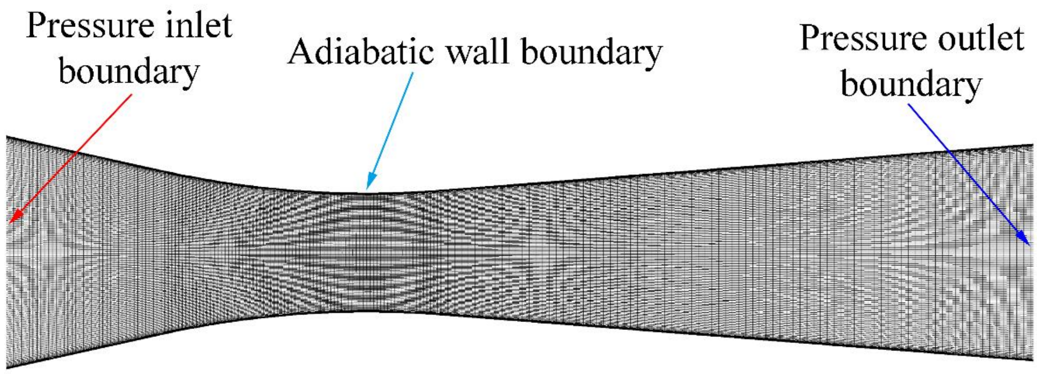

Fig. 2 Numerical modelling of CO_2 flow behaviour in supersonic flows: geometry, boundary conditions and grids

Table 1. Dimensions of the Laval nozzle

Geometrical parameters	Value (mm)
Diameter of nozzle inlet	62.90
Diameter of nozzle throat	21.60
Diameter of nozzle outlet	42.42
Length of nozzle converging part	93.30
Length of nozzle diverging part	198.58

Table 2. Operating conditions for the numerical modelling of CO_2 condensation in

supersonic flows

Inlet conditions	Outlet conditions	Wall conditions
Total pressure: 40 bar Total temperature: 293.15 K	Supersonic flows	No-slip, adiabatic wall

3 Mathematical modelling

3.1 Governing equations

This study focuses on the condensation behaviour of CO_2 condensations in supersonic flows. Considering the small size of the condensed droplets, it is assumed that the droplets follow the gaseous phase streamlines and there is no slip velocity between the two phases [27]. Hence, the single-fluid model is used in this study and the compressible Navier-Stokes equations are applied to govern the average mixture fluid as follows [28].

$$\frac{\partial \rho}{\partial t}+\frac{\partial(\rho u_j)}{\partial x_j}=-\dot{m} \tag{1}$$

$$\frac{\partial}{\partial t}\left(\rho u_i\right)+\frac{\partial}{\partial x_j}\left(\rho u_j u_i\right)=-\frac{\partial p}{\partial x_i}+\frac{\partial \tau_{ij}}{\partial x_j}-u_i\dot{m} \tag{2}$$

$$\frac{\partial}{\partial t}(\rho H)+\frac{\partial}{\partial x_j}(\rho u_j H+p)=-\frac{\partial}{\partial x_j}(\lambda_{eff}\frac{\partial T}{\partial x_j})+\frac{\partial}{\partial x_j}(u_i\tau_{ij})-h_{lv}\dot{m} \tag{3}$$

where $\dot{m}$ is the condensation mass generation rate due to the phase change process of CO_2 in supersonic flows [29, 30]. To model the condensation process, the following two scalar equations are employed to describe the droplet number (n), and liquid fraction (y) [31]:

$$\frac{\partial(\rho n)}{\partial t}+\frac{\partial}{\partial x_j}\left(\rho n u_j\right)=\rho I \tag{4}$$

$$\frac{\partial(\rho y)}{\partial t}+\frac{\partial}{\partial x_j}\left(\rho y u_j\right)=\dot{m} \tag{5}$$

The SST *k*-*ω* turbulence model [32, 33] was suggested for the prediction of the condensation phenomenon in transonic flows [34].

$$\frac{\partial}{\partial t}(\rho k)+\frac{\partial}{\partial x_i}(\rho k u_i)=\frac{\partial}{\partial x_j}\left(\Gamma_k \frac{\partial k}{\partial x_j}\right)+\bar{G}_k-Y_k+S_k \tag{6}$$

$$\frac{\partial}{\partial t}(\rho\omega)\frac{\partial}{\partial x_j}(\rho\omega u_j)=\frac{\partial}{\partial x_j}\left(\Gamma_\omega \frac{\partial \omega}{\partial x_j}\right)+C_\omega-Y_\omega+D_\omega+S_\omega \tag{7}$$

where Γ_k and Γ_ω are the effective diffusivity of k and ω, respectively.

3.2 Condensation process in supersonic flows

This condensation of CO_2 in supersonic flows includes the homogeneous nucleation process and droplet growth process. The equation (8) describes the nucleation rate due to the homogeneous nucleation process while the equation (10) was employed to calculate the droplet growth process.

$$I=\frac{q_c}{1+\phi}\frac{\rho_v^{\,2}}{\rho_l}\sqrt{\frac{2\sigma}{\pi m_v^{\,3}}}\exp\left(-\frac{4\pi\sigma}{3k_B T_v}r_c^{\,2}\right) \tag{8}$$

$$\phi=2\frac{\gamma-1}{\gamma+1}\frac{h}{R_v T_v}\left(\frac{h}{R_v T_v}-\frac{1}{2}\right) \tag{9}$$

$$\frac{dr}{dt}=\frac{\lambda_v\left(T_s-T_v\right)}{\rho_l h_{lv} r}\frac{\left(1-r_c/r\right)}{\left(\frac{1}{1+2\beta\mathrm{Kn}}+3.78(1-\nu)\frac{\mathrm{Kn}}{\mathrm{Pr}}\right)} \tag{10}$$

$$\nu=\frac{RT_s}{h}\left(\alpha-0.5-\frac{2-q_c}{2q_c}\left(\frac{\gamma+1}{2\gamma}\right)\left(\frac{c_{pv}T_s}{h}\right)\right) \tag{11}$$

where I and dr/dt are the nucleation rate and droplet growth rate [35, 36]. The modelling parameters used in this study include q_c = 1.0, α = 1.0, β = 0.0. The condensation mass generation rate $\dot{m}$ is contributed by two parts from the nucleation process and droplet growth process, which can be expressed as follows

$$\dot{m} = \frac{4\pi r_c^3}{3}\rho_l I + 4\pi r^2 \rho_l n \frac{dr}{dt} \tag{12}$$

The numerical simulation is carried out based on ANSYS Fluent 18.2, while the scalar equations (4) and (5) to describe the phase change process was integrated into Fluent using User-Defined-Scalar (UDS) and User-Defined-Function (UDF) interfaces. The droplet number and liquid fraction are solved by two additional scalar equations by UDS, while the source terms are employed to describe the mass generation during nonequilibrium condensations in transonic flows by UDF. The pressure inlet and pressure out boundaries are assigned to the entrance and exit of supersonic nozzles. The convergence criteria are below 1.0×10^{-4} for all dependent variables and the relative difference of mass flow rate between the inlet and out boundaries is lower than 0.0005%.

4 Results and discussion

4.1 Model validations

4.1.1 CFD model validation

The developed CFD model is validated against the non-equilibrium condensation in the Gyarmathy's nozzle [37] under high-pressure conditions. The total pressure and total temperature in experimental tests are 89 bar and 619.96 K, respectively. The heights of the nozzle throat and nozzle exit are 10.00 mm and 17.91 mm, and the detailed dimension is shown in Fig. 3 (a). Fig. 3 (b) – (d) describe numerical contours and profiles of static pressure and droplet radius inside Gyarmathy's nozzles [37]. The comparisons between numerical and experimental data demonstrate that the numerical model not only captures the condensation shock, but also accurately predict the droplet growth process with a maximum relative error of the droplet radius of approximately

15%. It demonstrates that our condensing flow model accurately computes the nonequilibrium condensation within supersonic flows.

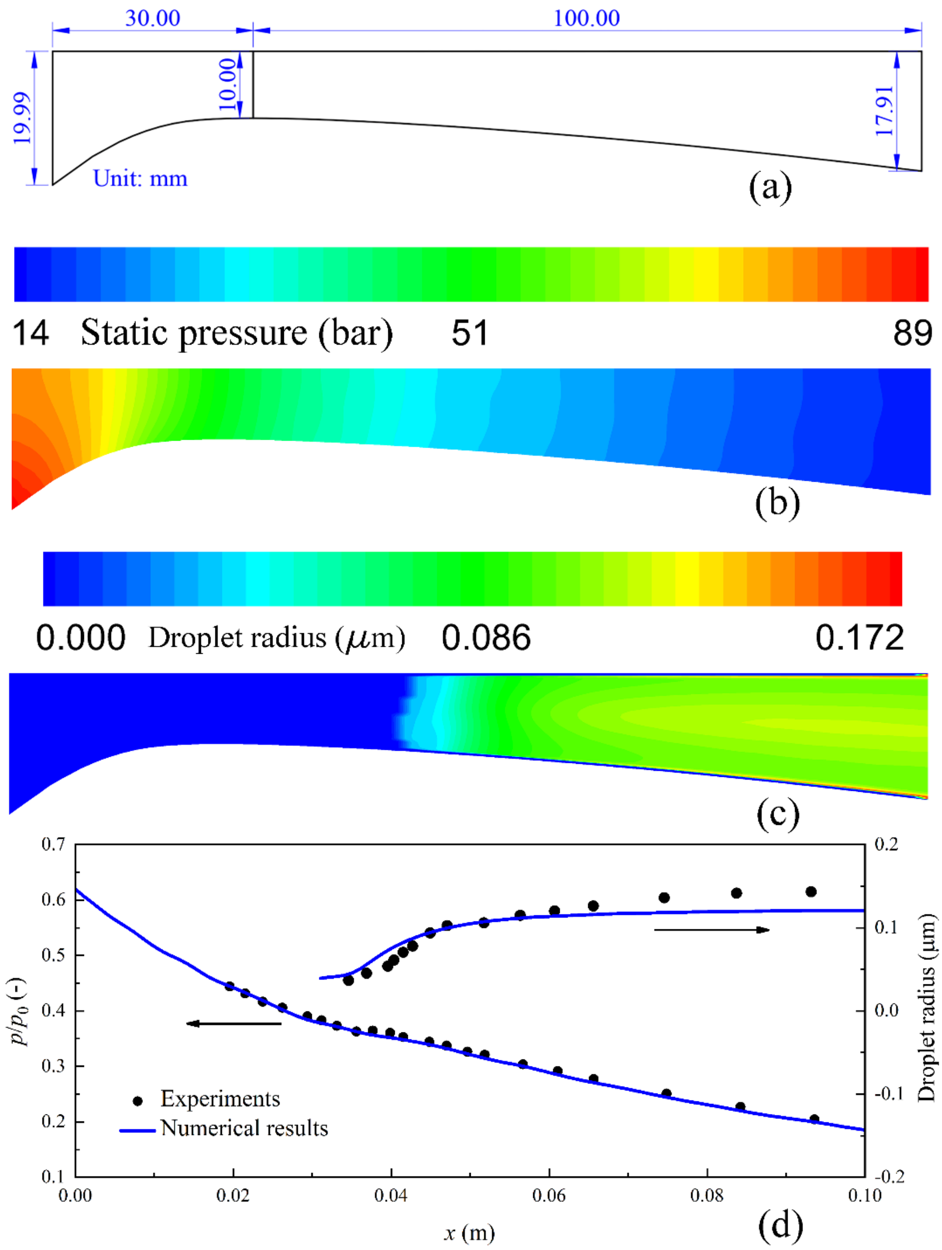

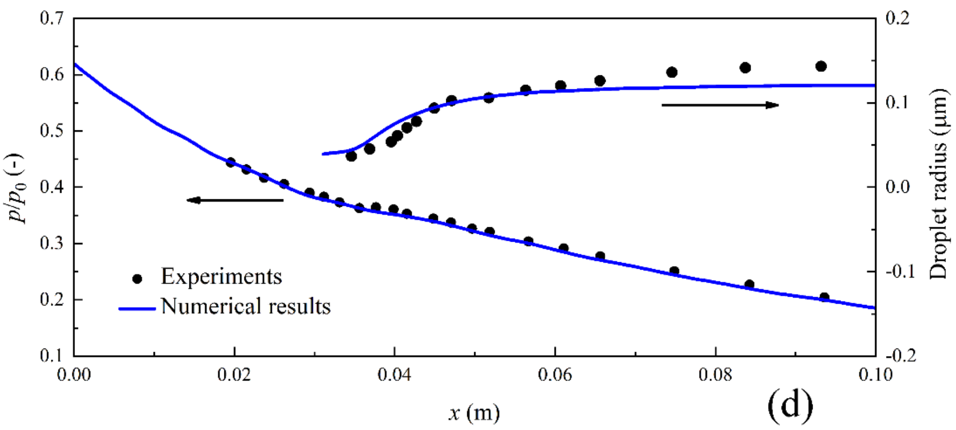

Fig. 3 Model validation against the Gyarmathy's nozzle [37]

4.1.2 Mesh independent tests

The complicated flow phenomenon for the CO_2 phase transition in supersonic flows, such as transonic flows, boundary layer separation, nucleation process and droplet growth process, requires a suitable grid density for the numerical simulation. The global flow structure, i.e. Mach number and condensation parameter, i.e. liquid fraction is used to study the influence of grid densities. The mesh independent test is carried out based on three different grid densities of 13600 (coarse mesh), 29400 (medium mesh), and 61100 (fine mesh) structured cells, respectively. Fig. 4 shows Mach number and liquid fraction along with flow directions and at the nozzle exit plane. We can see that the static pressure and liquid fraction along the flow direction are extremely similar for three different grid densities. For instance, all three different grid densities predict the Mach number of 1.77 and liquid fraction of 0.28 at the centre of the nozzle outlet. For the longitudinal distribution at nozzle exit planes, the coarse mesh represents the divergence both for Mach numbers and liquid fractions in near-wall regions compared to medium and fine meshes, while these two compute similar Mach numbers and liquid fractions. Therefore, the medium mesh is utilised for CO_2 nonequilibrium condensations within supersonic flows considering numerical accuracies and computational costs.

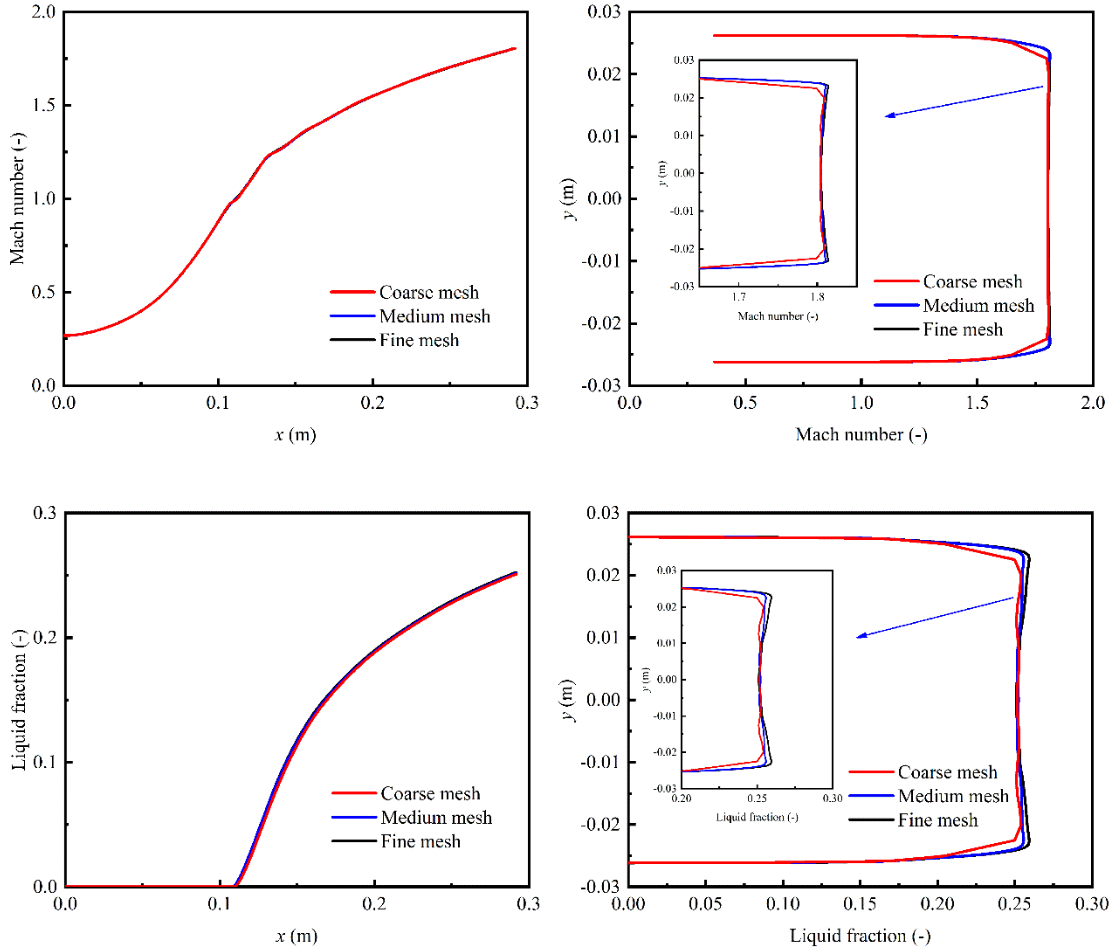

Fig. 4 Effect of mesh density on CO_2 nonequilibrium condensation

4.2 Effect of thermodynamics model on flow rates

The processing capacity is the primary factor in evaluating the working performance for CO_2 removal using supersonic flows. For evaluation of mass flow rates, it is assumed that choked flows are reached inside Laval nozzles, which means that fluid flows reach critical conditions at nozzle throats. Based on the ideal gas law, the mass flow rate can be calculated:

$$M = \rho_0 v_0 A_0 = \rho_{th} v_{th} A_{th} \tag{13}$$

where ρ_0, v_0 and A_0 are the fluid density, velocity and cross-section area at nozzle inlets.

ρ_{th}, v_{th} and A_{th} are the critical density, critical velocity and cross-section area at throats, M is mass flow rate.

The relationship between stagnation and critical parameters can be described using the ideal gas law:

$$p_0 = \rho_0 R T_0 \tag{14}$$

$$T_0 = (1+\frac{\gamma-1}{2})T_{th} \tag{15}$$

$$\rho_0 = (1+\frac{\gamma-1}{2})^{(\frac{1}{\gamma-1})}\rho_{th} \tag{16}$$

$$a_{th} = \sqrt{\gamma R T_{th}} \tag{17}$$

where γ is specific heat ratio. T_{th} and a_{th} are fluid temperature and sound speed at nozzle throats. p_0 and T_0 are the stagnation pressure and stagnation temperature, respectively.

Substituting relationships (14)-(17) into Eq. (13), the mass flow rate is expressed as:

$$M = \sqrt{\gamma}(\frac{2}{\gamma+1})^{\frac{\gamma+1}{2(\gamma-1)}}\frac{p_0}{\sqrt{RT_0}}A_{th} \tag{18}$$

Eq. (18) shows that the specific heat ratio dominates the mass flow rate for choked nozzle flows, while the statice pressure and temperature are constant at nozzle inlets.

A compressibility factor is usually considered as an indicator of the deviation from the ideal gas assumption. Fig 5 (a) and (c) displays the contour and profile of the compressibility factor based on the Redlich – Kwong EOS for CO_2. It shows that the compressibility factor varies from 0.75 at the nozzle inlet to 0.95 at the nozzle exit. The deviation from the ideal gas law results in inaccurate predictions of the heat and fluid flow inside high-pressure supersonic flows. Fig 5 (b) and (c) represent the specific heat ratio predicted by ideal gas and Redlich – Kwong real gas models. The specific heat ratio increases along the flow direction in the Laval nozzle using the Redlich – Kwong EOS, while the ideal gas law gives a constant value of 1.287. The specific heat ratios from Redlich -Kwong EOS are less than the ones calculated by an ideal gas model. The relative error of the specific heat ratio between the two models is 7.54% at the nozzle throat under the condition of the inlet pressure of 40 bar.

Fig 5 (d) shows the influence of the ideal gas assumption and Redlich - Kwong model on CO_2 mass flow rates through nozzles under various inlet pressures from 30 bar to 50 bar. The predicted mass flow rate of the ideal gas assumption significantly deviates from the real gas model. As expected, the relative error between the two models increases with the rise of the inlet pressure. The relative error exceeds 10% with the inlet pressure more than 30 bar, which reaches 25% at 50 bar. It indicates that the ideal gas assumption immensely under-predicts CO_2 mass flow rates through a Laval nozzle.

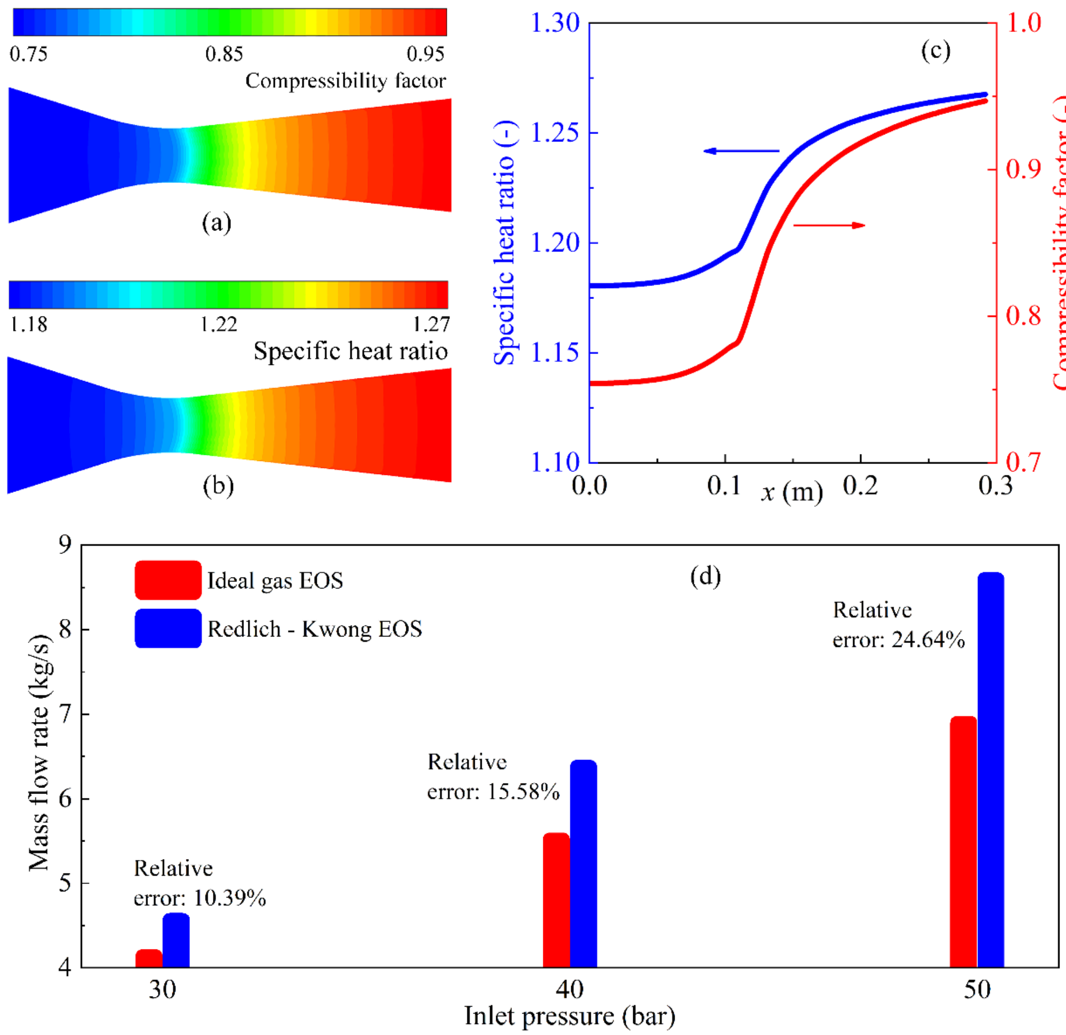

Fig. 5 Compressibility factor (a, c), specific heat ratio (b, c) and mass flow rate (d) of CO_2 in supersonic flows

4.3 Effect of thermodynamics model on flow structures

Fig. 6 depicts the contours and profiles of the gas velocity, sound speed and Mach number of CO2 in the Laval nozzle. Both ideal gas and Redlich – Kwong model reach choked flows of CO_2 in the Laval nozzle. The fluids accelerate inside the converging part, reach critical conditions at the throat and achieve supersonic flows inside the diverging part. However, the ideal gas assumption predicts a larger velocity, sound speed and Mach number than the Redlich – Kwong EOS during the phase transition of

CO_2 in supersonic flows. The distribution of Mach number in Fig. 6 (c) demonstrates that the relative error between the two models becomes more apparent in the diverging part of the Laval nozzle, where a further expansion of CO_2 occurs. For instance, the ideal gas and Redlich – Kwong model predict the Mach number of 1.94 and 1.77 at the nozzle exit, resulting in a relative error of approximately 9.6%. It means that the expansion characteristics of the CO_2 in the Laval nozzle are over-predicted by the ideal gas assumption.

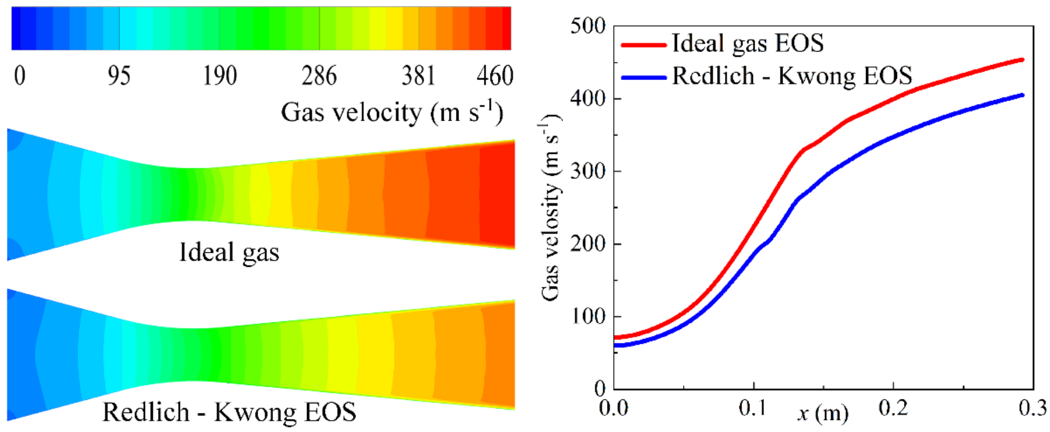

(a)

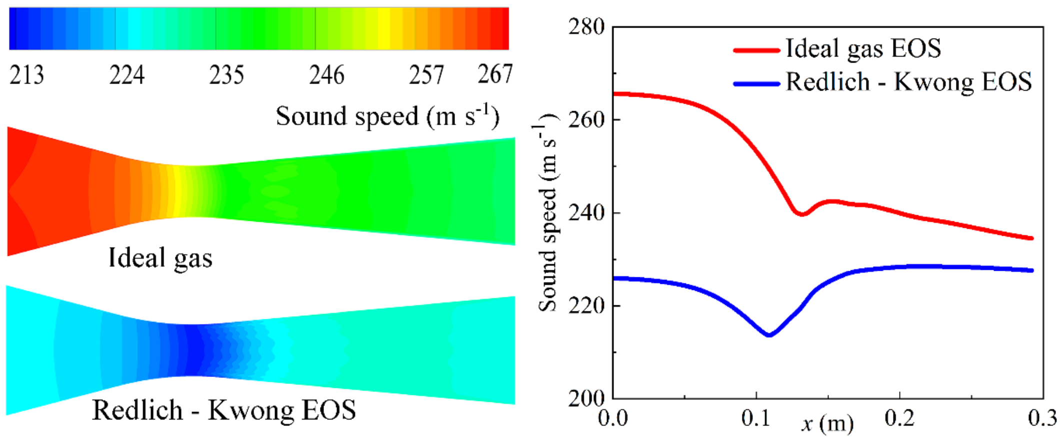

(b)

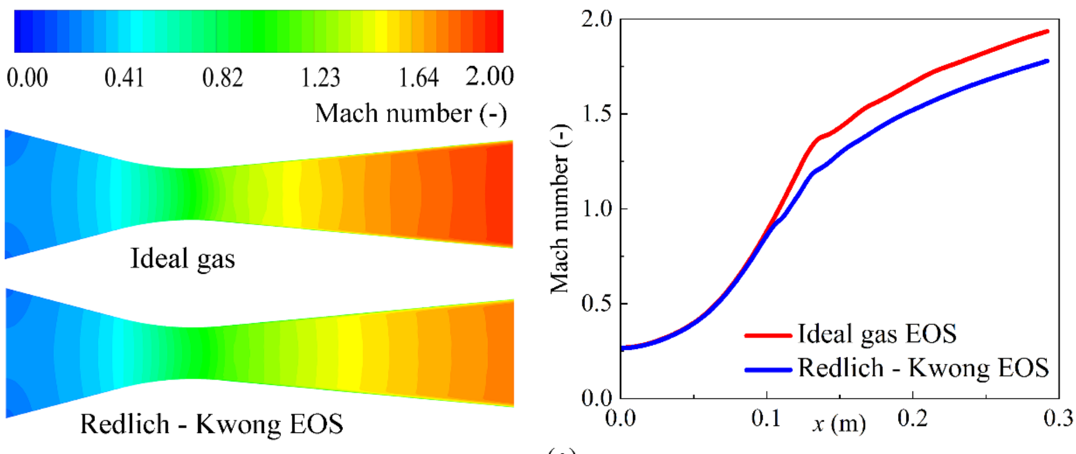

(c)

Fig. 6 Gas velocity (a), sound speed (b) and Mach number (c) in the Laval nozzle

Fig. 7 depicts static pressure and static temperature of CO_2 in the Laval nozzle based on ideal gas and Redlich – Kwong models. It can be observed that the two models both predict the condensation shock because of the phase transition in supersonic flows. This indicates that these two models accurately capture the heat and mass transfer which represent the heating effect due to latent heat release during the formation of liquid droplets. The higher static pressure and temperature from the Redlich – Kwong EOS than ideal gas model inside the diverging part also demonstrate that an ideal gas law overpredicts the expansion characteristic. Furthermore, the different position of the condensation shock represents that the ideal gas assumption computes a later onset of CO_2 nonequilibrium condensations inside supersonic flows compared to Redlich – Kwong EOS.

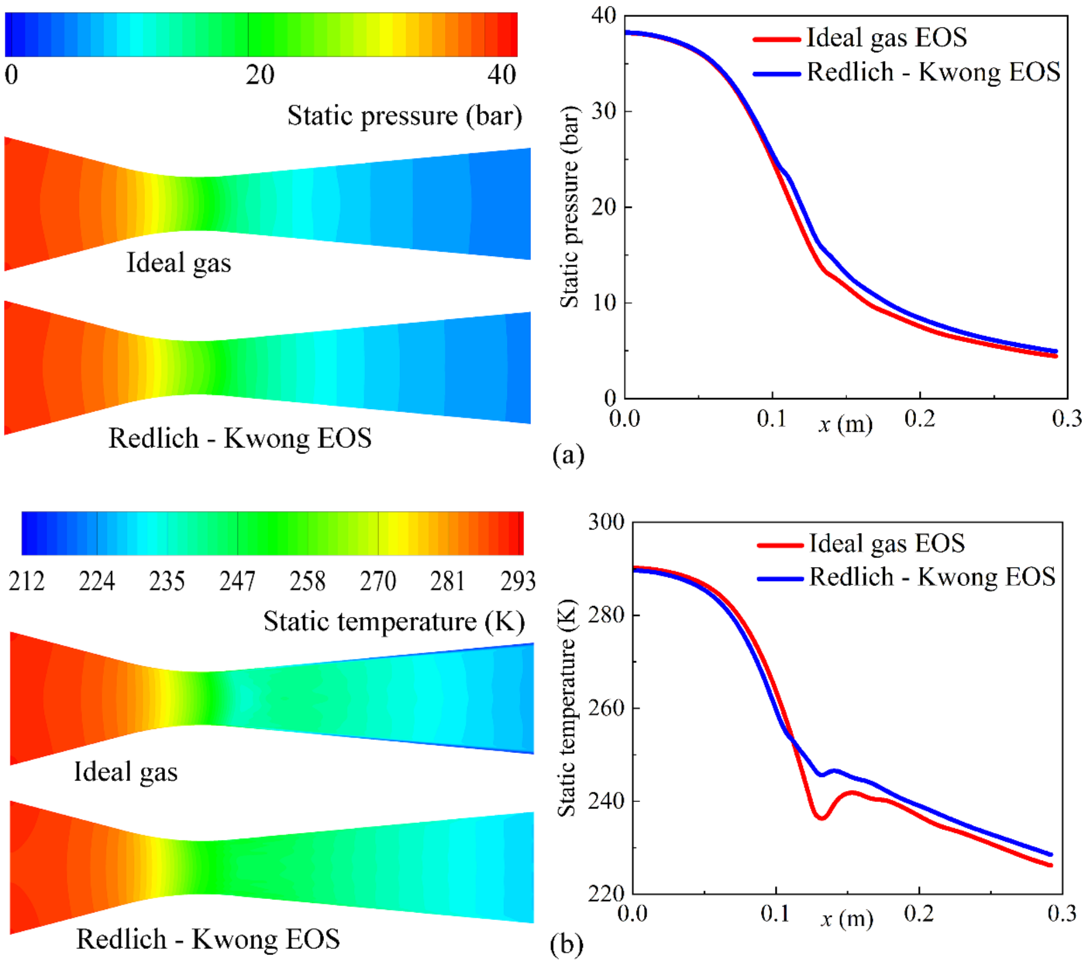

Fig. 7 Static pressure (a) and temperature (b) in supersonic nozzles

4.4 Effect of thermodynamics model on condensation features

The mass generation during the phase change determines the heat mass transfer between gaseous and liquid phases of CO_2 condensations within supersonic flows. Fig. 8 represents contours and profiles of two contributions to the mass generation in the nucleation process, $\dot{m}_1$ and droplet growth process, $\dot{m}_2$. It can be observed that the ideal gas assumption and Redlich – Kwong EOS predict tremendous different positions of the starting point of the mass generation both due to the nucleation and droplet growth processes. The Redlich – Kwong EOS shifts upward the starting point of the mass generation to the nozzle throat. Taking the mass generation due to the nucleation process, $\dot{m}_1$ as an example, the Redlich – Kwong real gas model computes the starting point at x = 0.105 m while the ideal gas gives the position at x = 0.121 m. Furthermore, the Redlich – Kwong EOS predicts higher mass generation both for the nucleation and droplet processes than the ideal gas assumption. For example, the maximum mass generation in the nucleation process, $\dot{m}_1$ by the Redlich – Kwong EOS is approximately 5.8 x 10^{-5} kg m^{-3} s^{-1} compared to the maximum 3.8 x 10^{-5} kg m^{-3} s^{-1} calculated by the ideal gas at the central line. For the mass generation in the droplet growth process, $\dot{m}_2$, the ideal and real gas models predict a maximum value of 2.6 x 10^4 kg m^{-3} s^{-1} and 4.5 x 10^4 kg m^{-3} s^{-1}, respectively.

When looking closely at the detail of the starting point of the mass generation in the nucleation $\dot{m}_1$ and droplet growth processes $\dot{m}_2$, both the ideal gas and Redlich – Kwong EOS represent similar predictions that the $\dot{m}_1$ starts upstream the $\dot{m}_2$. Taking the real gas model, for example, the $\dot{m}_1$ starts at x = 0.121 m compared to x = 0.125 m for the $\dot{m}_2$. This demonstrates that the nucleation process occurs first when a cluster of a critical droplet is formed and then the droplet grows on the surface of the critical droplet. In addition, there are 9 orders of magnitude between the mass generation in the nucleation process $\dot{m}_1$ and the droplet growth process $\dot{m}_2$, which indicates that the droplet growth process contributes significantly to the mass transfer in CO_2 condensations in supersonic flows.

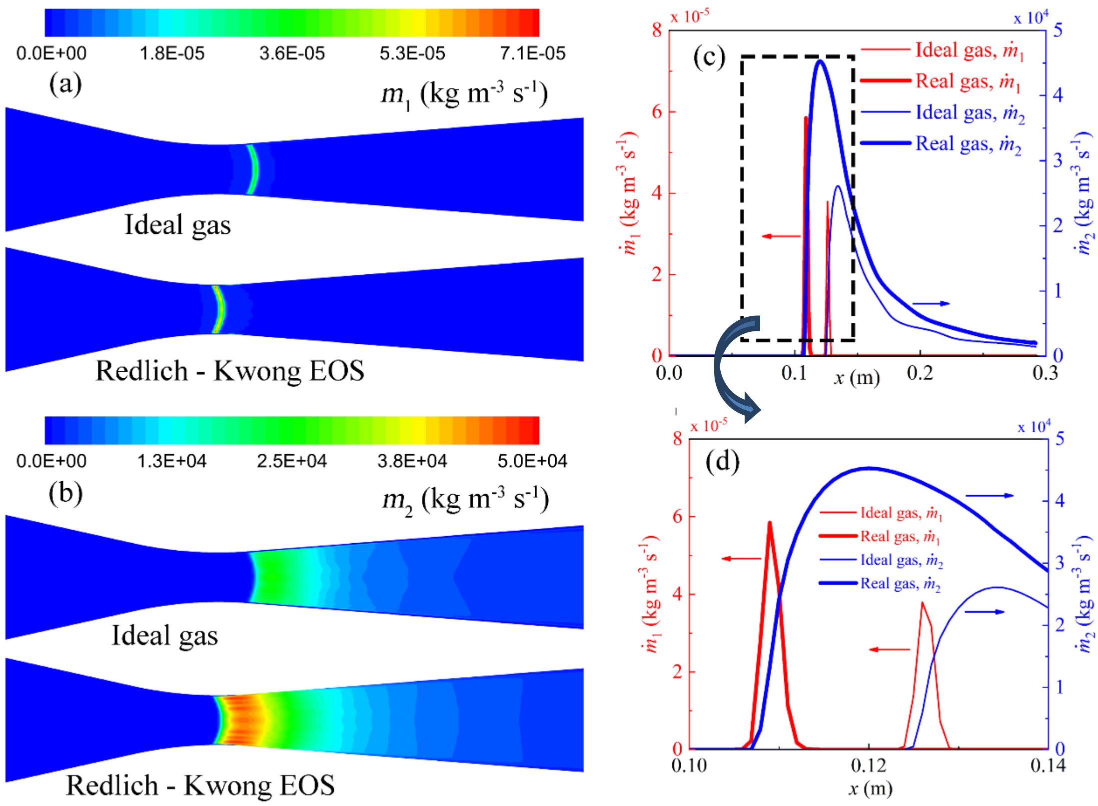

Fig. 8 Mass generation for CO_2 condensations inside supersonic flows

Fig. 9 depicts the nucleation rate of CO_2 phase transitions in supersonic flows. It can be seen that the distribution of the nucleation rate looks extremely similar with the mass generation due to the nucleation process both for the ideal gas model and Redlich – Kwong EOS. The nucleation process generates numerous nuclei in an exceedingly short time, which results in a sharp increase first and then an abrupt decrease of the mass generation $\dot{m}_1$. The ideal gas and Redlich-Kwong models compute the different onsets of non-equilibrium condensation of CO_2, although both of them predict a similar maximum nucleation rate of approximately 1.5 x 10^{18} m^{-3} s^{-1}.

Furthermore, the effect of the thermodynamics model on the droplet radius of CO_2 in supersonic flows is described in Fig. 10 based on the real gas model and ideal gas assumption. It can be seen that the real gas model predicts higher droplet radius than the ideal gas model. The droplet radius can reach 0.84 μm for the real gas model while the ideal gas assumption only calculates 0.30 μm. This means that the ideal gas assumption underpredicts the generation of the droplet diameters during the CO_2 condensation in supersonic flows. Fig. 11 shows that the thermodynamic model significantly determines the liquid fraction. The ideal gas model under-predicts the CO_2 condensation of 15% of the total mass in liquid fractions, while Redlich-Kwong EOS predicts liquid fractions of 28% of the total mass. Taking the Redlich – Kwong EOS as an example, the total liquid fraction due to the nucleation process is approximate 1.3 x 10^{-13}. This indicates that the contribution of the mass generation in the nucleation process $\dot{m}_1$ to the total liquid mass fraction is far from the contribution due to the droplet growth process $\dot{m}_2$.

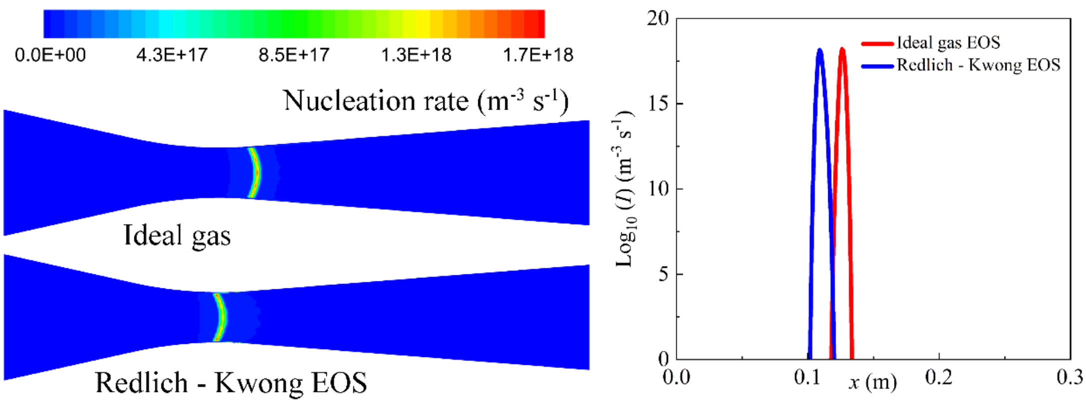

Fig. 9 Nucleation rates for CO_2 condensation inside supersonic flows

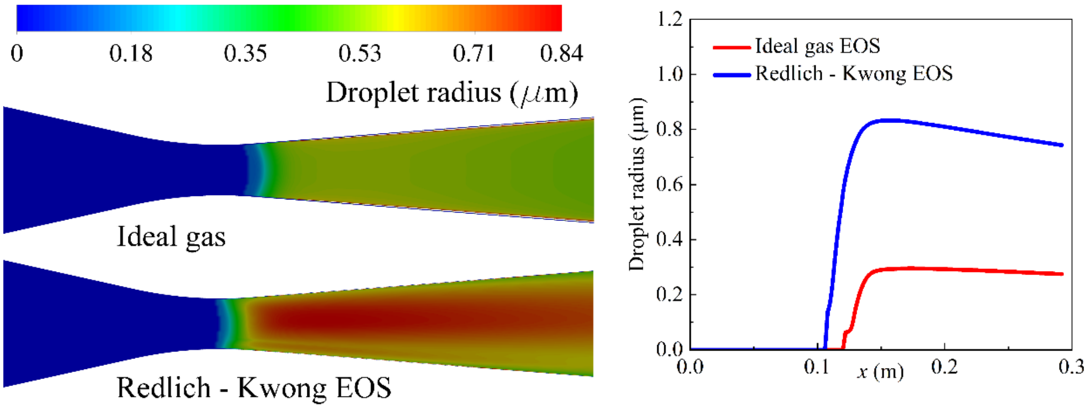

Fig. 10 Droplet radius for CO_2 condensation in supersonic flows

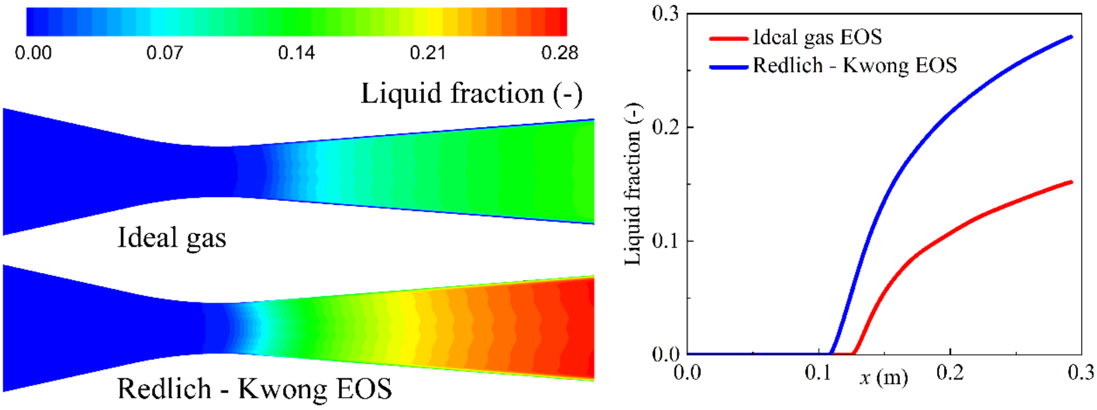

Fig. 11 Liquid fraction for CO_2 condensation in supersonic flows

4.5 Discussion

This study evaluates the potential of CO_2 separation in supersonic flows using the computational dynamics modelling approach. There are a few questions that need to be clarified here. The first question is about the validation of the developed numerical model in this study. Currently, there are no sufficient experimental data available for the nonequilibrium condensation of CO_2 in supersonic flows. Hence, it is very hard to validate the developed CFD model using CO_2 as the working fluid at the current stage. Instead, we employ the water vapour as a working fluid to carry out the validations of our numerical model. As the design of this study is for offshore natural gas processing, similar operating conditions at a high inlet pressure are utilised in a supersonic nozzle for the validation of the developed numerical model, in which both the pressure distribution and droplet size are available in the experimental measurements carried out by Gyarmathy [37]. For this case of water vapour, the comparison shows a good agreement between the numerical and experimental results, which demonstrates the accuracy of the developed condensing flow model for the prediction of the phase change behaviour of a condensable fluid in supersonic flows. In future studies, it is expected to conduct experimental studies to measure the pressure distribution as well as the droplet size or liquid fraction during the CO_2 condensation in supersonic nozzles. The experimental measurements will not only provide solid evidence for the potential of CO_2 removal in supersonic flows, but also will be very helpful for the numerical evaluation of this new concept by providing a useful database for the validation of the numerical model.

The second question is the advantage of this new concept of CO_2 removal using the nonequilibrium condensation in supersonic flows. It would be more relevant if the supersonic condensation-based separation technology could be compared with other physical processes such as commercially available membranes and cryogenic separation that can take advantage of high pressure gas streams. Although we have not carried out a detailed quantitative analysis for this proposed concept, the qualitative analysis is performed here to clarify the advantage of this new concept. Firstly, this new concept is oriented for offshore natural gas processing, where the operating condition from a natural gas well is at high pressure. When the high-pressure natural gas is introduced to the inlet of the new supersonic separation system, the pressure difference between the inlet and outlet will drive the gas mixture to go through the tubular device. A Laval nozzle inside the tubular device ensures the production of a supersonic flow for the nonequilibrium condensation of condensable components. Therefore, this new tubular concept does not consume external energy and cost to achieve the supersonic flows. Instead, this new technology can maximise the use of high pressure from the gas well to save energy, which is usually wasted in a throttling valve installed in current offshore natural gas processing systems. Secondly, the new concept is designed into a tubular device which ensures a small size and lightweight equipment. This is important for an offshore platform considering the limited space. This will ensure to easily install and integrate the new tubular equipment to an offshore natural gas processing system. Thus, the new concept will save huge capital costs compared to other CO_2 separation technologies. Lastly, on the one hand, the new concept enables high reliability as there is no rotating in this tubular device. On the other hand, there is no need to use chemicals to prevent hydrate during natural gas processing. These two advantages can significantly reduce the operating fees for CO_2 removal in supersonic flows. Therefore, the proposed new concept will present a competitive role compared to conventional CO_2 separation technologies.

The third question is the separation performance of CO_2 removal in supersonic flows. However, it cannot be evaluated in this study due to the pure CO_2 stream is assumed and the swirling flow is not considered in this simulation. Considering the working principle of this new concept, the separation performance depends on the condensation behaviour of CO_2 in supersonic flows and the swirling flow to remove the condensed droplets from the gas mixture. The present numerical studies demonstrate the potential of the nonequilibrium condensation of CO_2 in supersonic flows. For the next step, we need to optimise the structure of the swirling flow generators to achieve a strong swirling flow, which will be expected to generate a powerful centrifugal force to remove the condensed droplets. The separation performance can be evaluated based on the modelling of the condensation and swirling flow behaviour. Based on the experience for the removal of water vapour in supersonic separators, Prast et al. [38] simulated an experimental-tested supersonic separator and found that the maximum tangential velocity was approximately 240 m/s to remove the maximum droplet diameter of water of around 1.2 μm – 1.8 μm. In our simulations, the maximum droplet diameter of CO_2 is 1.68 μm (0.84 μm for droplet radius), the supersonic separator is expected to reach tangential velocities of 200 m/s which can be achieved by optimising the swirling flow generator for a high separation performance.

5 Conclusions

This study examines the potential of CO_2 capture from gases using nonequilibrium condensations inside supersonic flows. This new concept achieves energy conversion and utilisation in a friendly-environmental way to mitigate CO_2 emission and contribute to climate change. This is accomplished by employing the nucleation dynamics, droplet growth model and real gas model to evaluate the nonequilibrium condensation process of CO_2 because of high expansions in supersonic flows.

The comparison between the ideal gas law and Redlich – Kwong EOS shows that an ideal gas assumption significantly underpredicts CO_2 mass flow rates through the Laval nozzle with a relative error of up to 25%. The expansion characteristics of CO_2 inside supersonic flows are over-predicted by ideal gas assumptions, i.e. Mach number of 1.94 at nozzle outlet by ideal gas law compared to 1.77 by Redlich – Kwong real gas model. Furthermore, the ideal gas assumption computes a later onset of CO_2 nonequilibrium condensations inside supersonic flows compared to real gas models. The Redlich – Kwong EOS predicts higher mass generation both for nucleation and droplet growth processes than ideal gas assumptions. There are 9 orders of magnitude between the mass generation in nucleation and droplet growth processes, which indicates that the droplet growth process contributes significantly to the mass transfer in CO_2 condensations inside supersonic flows. The ideal gas assumption under-predicts the liquid fractions of 15% of the total mass, while Redlich-Kwong EOS predicts liquid fractions up to 28% of the total mass.

The simulation work in the present study assumes a pure CO_2 stream, rather than a gas mixture, to assess the non-equilibrium condensation of CO_2 in a supersonic flow to evaluate the potential of CO_2 removal from offshore natural gas. As a result, the simulation is not representative of the condensation separation process which involves various gas properties, total pressure, and total flow rate that are different from pure CO_2 stream. Therefore, as a modelling study for a gas separation technology, a gas mixture such as a simplified mixture of methane and CO_2 (from which CO_2 is separated) should be considered in future studies.

Data Availability Statement: The research data supporting this publication are provided

within this paper.

References

[1] Zhang Z, Wang T, Blunt MJ, Anthony EJ, Park A-HA, Hughes RW, et al. Advances in carbon capture, utilization and storage. Applied Energy. 2020;278:115627.

[2] Zhang Z, Pan S-Y, Li H, Cai J, Olabi AG, Anthony EJ, et al. Recent advances in carbon dioxide utilization. Renewable and Sustainable Energy Reviews. 2020;125:109799.

[3] Yan J, Zhang Z. Carbon Capture, Utilization and Storage (CCUS). Applied Energy. 2019;235:1289-99.

[4] Gabrielli P, Gazzani M, Mazzotti M. The role of carbon capture and utilization, carbon capture and storage, and biomass to enable a net-zero-CO_2 emissions chemical industry. Industrial & Engineering Chemistry Research. 2020;59:7033-45.

[5] Fazlollahi F, Bown A, Ebrahimzadeh E, Baxter LL. Transient natural gas liquefaction and its application to CCC-ES (energy storage with cryogenic carbon capture™). Energy. 2016;103:369-84.

[6] Li H, Tang Z, Li N, Cui L, Mao X-z. Mechanism and process study on steel slag enhancement for CO_2 capture by seawater. Applied Energy. 2020;276:115515.

[7] Ostovari H, Müller L, Skocek J, Bardow A. From Unavoidable CO_2 Source to CO_2 Sink? A Cement Industry Based on CO_2 Mineralization. Environmental Science & Technology. 2021;55:5212-23.

[8] Wang P-T, Wei Y-M, Yang B, Li J-Q, Kang J-N, Liu L-C, et al. Carbon capture and

storage in China's power sector: Optimal planning under the 2° C constraint. Applied Energy. 2020;263:114694.

[9] Babar M, Bustam MA, Ali A, Shah Maulud A, Shafiq U, Mukhtar A, et al. Thermodynamic data for cryogenic carbon dioxide capture from natural gas: A review. Cryogenics. 2019;102:85-104.

[10] Huang W, Zheng D, Xie H, Li Y, Wu W. Hybrid physical-chemical absorption process for carbon capture with strategy of high-pressure absorption/medium-pressure desorption. Applied Energy. 2019;239:928-37.

[11] Myers TG, Font F, Hennessy MG. Mathematical modelling of carbon capture in a packed column by adsorption. Applied Energy. 2020;278:115565.

[12] Budhathoki S, Ajayi O, Steckel JA, Wilmer CE. High-throughput computational prediction of the cost of carbon capture using mixed matrix membranes. Energy & Environmental Science. 2019;12:1255-64.

[13] Mondal MK, Balsora HK, Varshney P. Progress and trends in CO_2 capture/separation technologies: A review. Energy. 2012;46:431-41.

[14] Babar M, Mukhtar A, Mubashir M, Saqib S, Ullah S, Quddusi AHA, et al. Development of a novel switched packed bed process for cryogenic CO2 capture from natural gas. Process Safety and Environmental Protection. 2021;147:878-87.

[15] Yun S, Oh S-Y, Kim J-K. Techno-economic assessment of absorption-based CO_2 capture process based on novel solvent for coal-fired power plant. Applied Energy. 2020;268:114933.

[16] Zhang Z, Cai J, Chen F, Li H, Zhang W, Qi W. Progress in enhancement of CO_2 absorption by nanofluids: A mini review of mechanisms and current status. Renewable Energy. 2018;118:527-35.

[17] Subraveti SG, Pai KN, Rajagopalan AK, Wilkins NS, Rajendran A, Jayaraman A, et al. Cycle design and optimization of pressure swing adsorption cycles for pre-combustion CO_2 capture. Applied Energy. 2019;254:113624.

[18] Lee S, Yun S, Kim J-K. Development of novel sub-ambient membrane systems for energy-efficient post-combustion CO_2 capture. Applied Energy. 2019;238:1060-73.

[19] Sun W, Cao X, Yang W, Jin X. Numerical simulation of CO2 condensation process from CH4-CO2 binary gas mixture in supersonic nozzles. Separation and Purification Technology. 2017;188:238-49.

[20] Cao X, Guo D, Sun W, Zhang P, Ding G, Bian J. Supersonic separation technology for carbon dioxide and hydrogen sulfide removal from natural gas. Journal of Cleaner Production. 2021;288:125689.

[21] Bian J, Jiang W, Hou D, Liu Y, Yang J. Condensation characteristics of CH_4-CO_2 mixture gas in a supersonic nozzle. Powder Technology. 2018;329:1-11.

[22] Hou D, Jiang W, Zhao W, Bian J, Liu Y, Lai X. Effect of linetype of convergent section on supersonic condensation characteristics of CH4-CO2 mixture gas in Laval nozzle. Chemical Engineering and Processing - Process Intensification. 2018;133:128-36.

[23] Chen J, Jiang W, Han C, Liu Y. Study on supersonic swirling condensation

characteristics of CO_2 in Laval nozzle. Journal of Natural Gas Science and Engineering. 2020;84:103672.

[24] Chen J, Jiang W, Han C, Liu Y. Numerical study on the influence of supersonic nozzle structure on the swirling condensation characteristics of CO2. Journal of Natural Gas Science and Engineering. 2021;88:103753.

[25] Vijayakumaran H, Lemma TA. CFD modelling of non-equilibrium condensation of CO_2 within a supersonic nozzle using metastability approach. Journal of Natural Gas Science and Engineering. 2021;85:103715.

[26] Jiang W, Bian J, Wu A, Gao S, Yin P, Hou D. Investigation of supersonic separation mechanism of CO_2 in natural gas applying the Discrete Particle Method. Chemical Engineering and Processing - Process Intensification. 2018;123:272-9.

[27] Yang Y, Karvounis N, Walther JH, Ding H, Wen C. Effect of area ratio of the primary nozzle on steam ejector performance considering nonequilibrium condensations. Energy. 2021;237:121483.

[28] Wen C, Ding H, Yang Y. Numerical simulation of nanodroplet generation of water vapour in high-pressure supersonic flows for the potential of clean natural gas dehydration. Energy Conversion and Management. 2021;231:113853.

[29] Kantrowitz A. Nucleation in very rapid vapor expansions. The Journal of Chemical Physics. 1951;19:1097-100.

[30] Young J. The spontaneous condensation of steam in supersonic nozzle. Physico Chemical Hydrodynamics. 1982;3:57-82.

[31] Wen C, Ding H, Yang Y. Optimisation study of a supersonic separator considering

nonequilibrium condensation behaviour. Energy Conversion and Management. 2020;222:113210.

[32] Menter FR. Two-equation eddy-viscosity turbulence models for engineering applications. AIAA journal. 1994;32:1598-605.

[33] Wen C, Karvounis N, Walther JH, Ding H, Yang Y. Non-equilibrium condensation of water vapour in supersonic flows with shock waves. International Journal of Heat and Mass Transfer. 2020;149:119109.

[34] Dykas S, Wróblewski W. Numerical modelling of steam condensing flow in low and high-pressure nozzles. International Journal of Heat and Mass Transfer. 2012;55:6191-9.

[35] Wen C, Karvounis N, Walther JH, Yan Y, Feng Y, Yang Y. An efficient approach to separate CO2 using supersonic flows for carbon capture and storage. Applied Energy. 2019;238:311-9.

[36] Yang Y, Zhu X, Yan Y, Ding H, Wen C. Performance of supersonic steam ejectors considering the nonequilibrium condensation phenomenon for efficient energy utilisation. Applied Energy. 2019;242:157-67.

[37] Gyarmathy G. Nucleation of steam in high-pressure nozzle experiments. Proceedings of the Institution of Mechanical Engineers, Part A: Journal of Power and Energy. 2005;219:511-21.

[38] Prast B, Lammers B, Betting M. CFD for supersonic gas processing. The Fifth International Conference on CFD in the Process Industries, Melbourne, Australia, 13-15 December, 2006.